Development and Applications of a Concentrating Membrane Osmometer for Colloid Solutions

Christopher S. Hale, Devin W. McBride, Ramsey Batarseh, Jordan Hughey, Kevin Vang, and V. G. J. Rodgers*

B2K Group (Biotransport & Bioreaction Kinetics Group)
Department of Bioengineering
University of California, Riverside, CA 92521 USA

Accepted March 6, 2019 to: Review of Scientific Instruments

*To whom correspondence should be addressed:
A127 Bourns Hall
University of California, Riverside
Riverside, CA 92521 USA
Telephone: 951-827-6241
Facsimile: 951-827-6416
E-mail: vrodgers@engr.ucr.edu

ABSTRACT

The membrane concentration osmometer coupled with multiple sample preparations has been used for over a century to determine a number of colloidal properties. At the dilute region, this method has been used to determine solute molecular mass. When the solution is proteinaceous, in the intermediate region, the osmotic pressure profile provides the second virial coefficient, useful for estimating protein crystallization and salting out. At the most crowded concentrations, it provides insight on protein hydration and protein-ion interaction. One of the most critical factors in generating the osmotic pressure profile is minimizing the quantity of protein used and reducing the error in preparing samples. Here, we introduce a membrane concentrating osmometer that allows one to measure osmotic pressure over a wide concentration range from a single sample. A test study was performed using the osmotic pressure profile of self-crowded bovine serum albumin (BSA) solutions. The resulting profile was in good agreement with previous data in the literature obtained from multiple sample studies. The osmotic pressure profile was further used with a free

solvent-based (FSB) osmotic pressure model to determine protein hydration and ion binding. These results were in excellent agreement with literature values. This concentrating osmometer has several advantages over conventional concentration osmometer for obtaining the osmotic pressure profile for proteinaceous solutions; 1) the amount of protein required is significantly decreased, 2) the potential for experimental error in sample preparation diminishes, and, 3) the time for generating the osmotic pressure profile is substantially reduced.

KEYWORDS: Osmometer, osmotic pressure, concentrating, crowded protein

INTRODUCTION

The use of osmometers to determine critical solution parameters dates back to the late nineteen century with van't Hoff's Nobel Prize-winning discovery that the relationship of osmotic pressure of dilute colloid solutions to concentration was consistent with the ideal gas law.[1,2] Researchers have subsequently used measured osmotic pressure for dilute solutions at various concentrations to extrapolate the molecular mass of a dissolved colloid.[3–6] It was soon recognized that van't Hoff's model could not account for the behavior of highly concentrated solutions and others offered the correction in the form of a phenomenological virial expansions that could account for solute-solute interactions.[7] This effort resulted in interpretations of the second virial coefficient as an interaction parameter.[8–14]

But in nearly all cases, the osmotic pressure results used in the interpretation of the solution properties requires a series of solutions of varying concentrations in the region of interest. This could be time intensive, both in preparation and in measurement. As examples, Vilker (1976) reported that each data sample used to generate the osmotic pressure profile required approximately 6 h to establish equilibrium using his manometer-based pressure measurement technique.[15] Because a minute but significant volume of fluid was transported across his two chamber osmometer, additional time was devoted to correcting for the final solvent- and solution-side concentrations.[15] Wu et al. (1999) indicated that, in their methods for preparing the osmotic pressure profile, each sample required overnight equilibration.[16] Yousef et al. (2001) reported that, in preparation of concentrated solutions of immune gamma globulin, dissolution of high concentrations required 2 or 3 days.[17] Yousef used a pressure transducer for the osmotic pressure measurements but the overall time for measurement equilibrium remained approximately 5-6 h.[17] Similar time requirements are reported in other studies where the osmotic pressure profile is generated.[18–21] Hale et al. (2018) modified the osmometer further by increasing the volume of the

solvent-side chamber of the device. This ultimately acted as an infinite sink and eliminated solution-side concentration corrections. Nevertheless, excessive sample preparation time and material use were not eliminated.[21] Overall, a time commitment on the order of days is required to generate a single osmotic pressure profile.

As eluded to above, the protein mass required to prepare each solution can also be significant. A single solution osmotic pressure data point in dilute solutions can require very little protein mass. However, for measurements at high concentrations, the solute mass can be on the order of grams.[17,22] Recent observations show that the osmotic pressure profile of highly concentrated self-crowded protein solutions provides insight into protein hydration and ion binding.[17,18,20,21,23–27] These are critical parameters in characterizing novel proteins. For many proteins of interest, the costs to providing gram quantities of protein to generate the osmotic pressure profile may be prohibitive. For self-crowded solutions studies, preparing an osmotic pressure profile can require substantial solution preparation and time.

Ultimately, the large time and materials commitment required to generate an osmotic pressure profile is relatively expensive. Because of this large investment, duplicate data points are rarely determined. Consequently, any error analysis is representative of the regression of the data to a proposed model.[15–17,21,23] An exception to this is the osmotic pressure profile for bovine serum albumin (BSA) in 0.7 M NaCl at pH 6.3 reported by Kappos and Pauly (1966).[28] These investigators showed error of as much as 15% in the osmotic pressure measurement for their highest concentration measurement. Vilker compared his osmotic pressure for BSA at 0.15 M NaCl and 5.4 pH and found his results to be as much as 25% lower than that of Kappos and Pauly but slightly higher than results obtained at 5.4 pH and 0.15 M NaCl by Scatchard.[29]

A number of innovations have been developed for the osmometer to reduce sample volume and increase measurement time.[22,30–36] However, no design to the authors' knowledge, address the reduction in sample preparation for each data point used in an osmotic pressure profile. One design has reduced the experimental time by incorporating a moderately large volume stirred cell, however, additional solute must be added to the system after each run to obtain measurements for different concentrations.[36] Here, we have designed and developed a concentrating osmometer that allows a single sample to be concentrated to provide the osmotic pressure profile used for solution property analysis. This is accomplished by beginning with an initial solution volume and after the osmotic pressure reaches steady state, decreasing the volume using a plunger, and then repeating these steps to obtain additional data points. Because the solution is nearly incompressible, the overall system is designed to withstand pressures much greater than the resulting osmotic pressure. This method also allows for a decrease in the time required to obtain a complete osmotic pressure-concentration curve. A conventional membrane osmometer requires that protein solutions be made for each desired concentration and wait sufficient time for a solution to reach steady state in the osmometer. As mentioned above, even when the pressure head is adjusted, this process can take hours per sample.[16] In this proposed design, working continuously with one initial solution and concentrating that solution repeatedly, the quantity of total sample mass is reduced and the time to obtain an osmotic pressure profile can be substantially decreased.

DESIGN OF THE CONCENTRATING OSMOMETER

Overall function

The concentrating osmometer is based upon the standard osmometer device which consists of two chambers, the solute chamber and the solvent chamber, separated by a supported semi-permeable membrane.[17–20,23] The membrane is such that the osmolyte of interest is totally retained. Selection of the membrane is important to ensure that only desired species are able to transverse

the membrane. This is achieved by selecting a membrane pore size that is large enough to freely allow permeability of the solvent, but small enough to prevent the restricted species from passing through. The membrane's chemical structure and all surfaces that come in contact with the species are selected to not affect the solutions.

Typically, a solution is added to the solute chamber and the solvent chamber is open to atmosphere. The solvent chamber is sufficiently large to represent an infinite sink. In the initial reading, the system is allowed to obtain equilibrium and the pressure reading is determined. The concentrating osmometer works by decreasing the solute chamber volume (Figure 1-A, yellow volume) to obtain new solute concentrations (Figure 1-B, yellow volume). By rotating the plunger (Figure 1-B, pink arrows) the volume in the solute chamber (Figure 1-B, yellow volume) is reduced, driving transmittable solvent through the semi-permeable membrane and into the solvent chamber (Figure 1-B, blue volume).

The difference in plunger height (Figure 1, ΔH), between before rotation (Figure 1-A, H_{P_1}) and the plunger height after rotation (Figure 1-B, H_{P_2}), is equivalent to the change in chamber height (Figure 1, ΔH) before (Figure 1-A, H_{C_1}) and after rotation (Figure 1-B, H_{C_2}). Knowing the dimensions of the solute chamber and assuming totally retained solutes, the change in chamber height can be used to determine the change in solute concentration by a mass balance. For the nth measurement, the concentration, c_n, is determined as

$$c_n = \frac{m_o}{V_o - \sum_{j=2}^{n} \Delta V_j}, \quad (1)$$

where m_o is the initial colloid mass in the sample, V_o is the initial sample volume, and ΔV_j is the volume change associated with the j^{th} measurement.

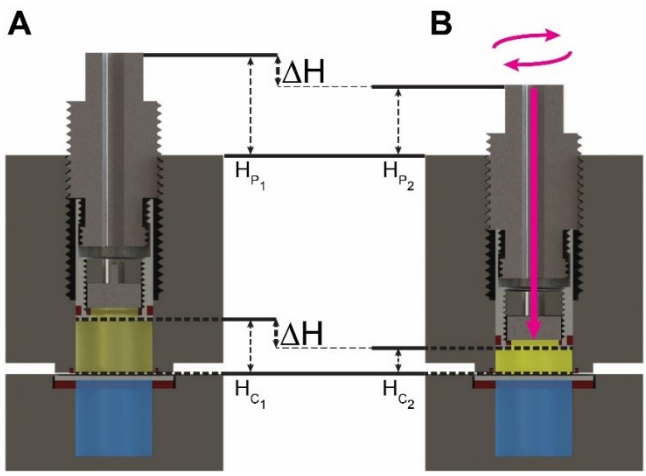

Figure 1: A collapsed view of the concentrating osmometer before (A) and after rotation (B). Rotation is denoted by the curved pink arrows in B), by which the solute chamber volume, denoted in yellow is decreased (pink arrow aimed down). The solvent previously in the protein solution before the rotation (A) is driven through a supported semi-permeable membrane into the solvent chamber denoted in blue. The solvent chamber is typically several orders of magnitude larger than the solute chamber and is open to atmosphere. The large capacity of the solvent chamber allows it to act as an infinite sink. The change in plunger height, ΔH, from its initial height, H_{P_1},to its new height, H_{P_2}, is equivalent to the change in chamber height, ΔH, from the initial height, H_{C_1}, to its end height, H_{C_2}. By knowing the change in chamber height and the dimensions of the chamber, the change in solute concentration is determined.

The overall device design is shown in Figure 2. During operation, the overpressure can become several times greater than the resulting osmotic pressure. Therefore, the device design was constructed to withstand pressures not normally present in conventional membrane osmometers. Details of the device measurements are shown in the supplement (Figures S1-S4). The following describes the details of the device.

Design of the solute chamber

The solute chamber (Figure 2 (7)) is a straight cylinder allowing for the maximum available membrane surface area. The solute solution is added directly into the solute chamber allowing for visual inspection and potential removal of any air pockets that may have developed during addition. Once enough solute has been added to form a meniscus above the solute chamber O-ring (Figure 2 (8)), the membrane is placed on top of the O-ring in such a way as to prevent air from

being trapped in the chamber. The detail of the design dimensions of the solute chamber are shown in the supplement (Figure S1).

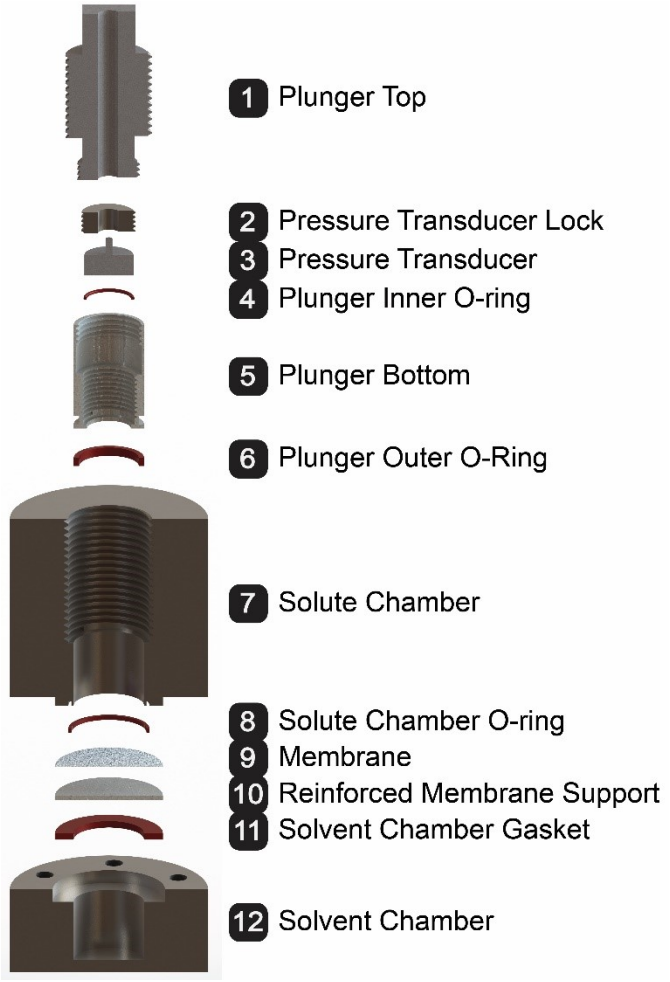

Figure 2: Exploded sectioned view of all the components in the concentrating osmometer. Components 1-6 represent the plunger that changes the solute volume and its O-rings (red – 4, 6) that seal off the solute chamber around the plunger. Component 7 and 12 are the solute and solvent chambers, respectively, with components 8-11 containing the components to allow transport between the chambers (9) and ensuring the two chambers are sealed (red - 8, 11).

Plunger design

In order to change the volume in the solute chamber, a plunger (Figure 2 (1-6)) is driven toward the membrane, increasing the pressure in the chamber and driving solute through the semi-permeable membrane, concentrating the remaining solute. The plunger is made up of two main sections, the lower (Figure 2 (2-6)) and upper components (Figure 2 (1)). The plunger bottom

(Figure 2 (5)) contains the pressure transducer (Figure 2 (3)). It is imperative that a pressure transducer is selected so that it provides the appropriate osmotic pressure reading for the sample range but is protected from the inevitable overpressure that occurs during the operation of the device.

The pressure transducer is designed to seal against the plunger to insure that there are no leaks. To achieve sealing, an O-ring (Figure 2 (4)) is placed around the sensing side of the transducer and the inside of the lower plunger. The transducer is secured against the O-ring with enough force to seal the chamber by a threaded cylindrical lock (Figure 2 (2)). The lock is screwed into the lower plunger to drive the transducer into the O-ring. The lock has a hole through the center with a slot cut from the center to the edge. This slot allows for the lock to slide over the transducer wires for ease of assembly. Due to the confined area, the slot is also the mechanism for which the lock is screwed. The slot allows for a flathead screw driver to slide through and then rotate to adjust the distance between the lock and the transducer.

The lower plunger also seals against the walls of the solute chamber. Another O-ring (Figure 2 (6)), around the diameter of the lower plunger, is used to ensure that solution does not leak around the plunger during concentrating and at elevated overpressures. This O-ring is located as close to the bottom of the lower plunger as possible while still allowing for most of the diameter to be enveloped on the top and bottom. The envelopment is important to support the O-ring when the plunger moves.

The upper component of the plunger threads into the solute chamber allowing the plunger to move up and down. The threading has been selected to maximize the vertical sensitivity while maintaining enough strength to ensure that the threads do not strip.

The plunger top and bottom are also connected by threading together, but with threads of the opposite direction of those connecting the solute chamber and the plunger top. These connections having opposing thread and a thread gap in the plunger connection, allow the two parts of the plunger to rotate independently of each other. This thread gap is after the connecting thread on both the plunger bottom and top, so that when the plunger is rotated to lower the plunger assembly deeper into the solute chamber, the threading between the plunger bottom and top are not in contact and so will prevent them from unthreading. Conversely, when the plunger assembly is unscrewed the threads of the plunger top and bottom come in contact but do not unscrew as the plunger top's rotation is in the opposite direction of the connecting threads. By constructing the plunger top and bottom in this way, the plunger assembly is only able to become disassembled outside of the osmometer.

The plunger top is slotted similarly to the transducer lock to allow the transducer wires to slide through for easy assembly. The slot has the added benefit of being useful as a measurement of rotation around the solute chamber. Given the plunger threading, initial location, and degree of rotation, the concentration of the solute solution can be determined by change in solute chamber height. In order to rotate the plunger, increasing or decreasing the solute chamber volume, the top of the upper plunger is notched allowing for attachment of a wrench. The design specifications of the plunger are shown in the supplement (Figure S2).

Solvent chamber

The solvent chamber (Figure 2 (12)) holds solution containing all transmittable species. In order to ensure that the transmission of species from the solvent to solute chamber does not significantly affect the concentration of that species on the solvent chamber, the quantity of solvent in the solvent chamber is several orders of magnitude larger, thus, acting as an infinite sink. Instead

of containing the large volume of solvent solution within the osmometer, the solvent chamber has a minimized volume, but ports are installed on the solvent side to pump solution past the membrane from a container of desired volume. Delivering solvent to the chamber, via a pump, has the added benefit of moving the solvent past the membrane by convection to reduce a diffusion boundary layer at the solvent side. The design dimensions for the solvent chamber are illustrated in the supplement (Figure S3).

Reinforced membrane support

The overpressure that results when contracting the solute solution has the potential to bow the membrane toward the solvent chamber, increasing the solute chamber volume, and, potentially, introducing error in the solute-side concentration calculation. To minimize this effect, a porous stainless-steel support (Figure 2 (10)) is employed on the solvent side of the membrane. The support is 1 mm thick with 3 mm circular openings separated by a nominal distance of 0.8 mm. The pores do not hinder the transmission of species and the overall support minimizes membrane flex. The membrane support is sealed around its diameter as well as on the solvent chamber side to prevent solution leaks. Sealing around the diameter can be achieved using non-reactive epoxy, while a gasket (Figure 1 (11)) can seal the membrane support to the solvent chamber. The detail dimensions of the membrane support are shown in the supplement (Figure S4).

Assembly

The solution and solvent chambers are screwed together in order to provide the pressure required to seal and secure the gaskets, between the solvent chamber, membrane support, membrane, and the solute chamber. In order to keep the membrane support and the gasket in line with the membrane and solvent chamber, the solvent chamber has a cutout for the gaskets and membrane support to rest, while the solute chamber has an extrusion of a slightly smaller diameter to ensure correct alignment and desired sealing pressure.

Concentrating factor

This design has a solute chamber with a maximum volume of 2.6 mL and a minimum volume of 140 μL. A total of 4.8 rotations of the plunger are required to cover the span of this volume range. The height change of each 360° rotation is 1.6 mm and there is a total change in the plunger tip height of 7.6 mm. This allows the solution of interest to be concentrated up to 18.9 times the initial concentration. The reduced volume and concentration range allows osmotic pressure profiles to be produced for relatively small samples of proteins. This is particularly advantageous for samples that are not available in gram quantities. As an example, in our previous standard osmometer, over 100g of protein were needed to generate a complete osmotic pressure profile. Whereas, the concentrating osmometer can produce an osmotic pressure profile for a concentration range between 21.2 gL^{-1} to 400 gL^{-1}, with only 55 mg of BSA.

Although this design is used herein to validate a concentrating osmometer, alterations can be made to the design to further reduce the minimum and maximum volumes to increase the concentrating factor as necessary.

EXAMPLE APPLICATION: PREDICTION OF HYDRATION AND ION BINDING OF SELF-CROWDED BSA

Overview

In this example, a single sample of BSA is used to generate an osmotic pressure profile that can be used to predict protein hydration and ion binding via the free solvent-based (FSB) osmotic pressure model.[17–20,23–25,27,37,38] These parameters can be extracted from the non-linear range of the osmotic pressure profile.

Free solvent-based (FSB) model relates osmotic pressure profile to hydration and ion binding

Full mathematical development of the free-solvent based model is described elsewhere.[17,25] Briefly, for a two chamber osmometer separated by a semi-permeable membrane in which there

are n distinct species, where p proteins (or other rejected solutes) are fully rejected and confined to chamber II and the remaining species (n - p) are diffusible, the free-solvent based model describes the osmotic pressure, π, as

$$\pi \approx \frac{RT}{\bar{V}_1}\ln\left(\frac{\left(\sum_{i=1}^{n} N_i^{\mathrm{II}} - \sum_{i=1;i\neq 2\to p+1}^{n}\sum_{j=2}^{p+1}\nu_{ij}N_j^{\mathrm{II}} - \sum_{j=p+2}^{n}\nu_{1j}N_j^{\mathrm{II}}\right)\left(N_1^{\mathrm{I}} - \sum_{j=p+2}^{n}\nu_{1j}N_j^{\mathrm{II}}\right)}{\left(N_1^{\mathrm{II}} - \sum_{j=2}^{n}\nu_{1j}N_j^{\mathrm{II}}\right)\left(\sum_{i=1}^{n} N_i^{\mathrm{I}} - \sum_{j=p+2}^{n}\nu_{1j}N_j^{\mathrm{II}}\right)}\right), \qquad (2)$$

where N_i^k is the number of moles of species i in compartment k, and ν_{ij} is the net number of moles of species i interacting with species j. The compartment containing the protein solution is denoted as superscript II, while the non-protein compartment is denoted as superscript i. For this work, in a self-crowded protein solution in a single salt, the total number of components is three; water, protein, and the salt, NaCl. The hydration, ν_{12}, and ion binding parameters, ν_{32}, are regressed from Eqn. (2) to best fit the osmotic pressure profile.

Experimental method

Solvent solutions are prepared by dissolving the designated mass of NaCl (No. S9888, Sigma-Aldrich, St. Louis, MO) into one liter of ultrapure water (EASYpure RoDi D13321, Thermo Scientific Barnstead Water System, Thermo Fisher Scientific, Waltham, MA) to produce a 0.15 M solution. This solvent is then used to dissolve a weighed mass of BSA (No. A30075, BSA, Research Products International, Mt Prospect, IL), using a stir bar to facilitate mixing. The solution pH of both solutions is measured by a pH Meter (Model 13-641-253, ThermoScientific Orion 720A+, Thermo Fisher Scientific, Waltham, MA) and adjusted, under stirring, using 1 M HCl (No. HX0603, Millipore Sigma, Burlington, MA) and 1 M NaOH (No. S318, Thermo Fisher Scientific, Waltham, MA), to be within 0.05 pH of the desired value. Stirring also allows for the prevention of local denaturation in the protein solutions. The amount of acid and base used to adjust pH is considered part of the solutions and is accounted for when calculating concentrations. The

concentration of the solutions was determined by dividing the amount of protein or salt by the volume of solvent used to make the solution. The volume of solvent includes volume of protein or salt in the solution using the specific volume of the protein or the density of the salt.

The general osmotic pressure experimental setup is equivalent to the design used for the standard membrane osmometer reported by Hale et al. (2018).[21] However, a single sample is used here to determine the concentration profile region of interest. Initially, a measured mass of the lowest concentrated solution is loaded into the solution chamber and the device is closed. Once assembled, and once the pressure reading stabilized, the pressure (Cole-Palmer, pressure transducer, EW-68001-04, Vernon Hills, IL) and plunger height (Electronic Digital Caliper, ± 0.0005 in resolution, ± 0.001 in accuracy) were recorded. The plunger was then rotated to reduce the solute chamber volume. Solvent, but not protein, is slowly expelled into the solution chamber. The solution chamber has a significantly larger volume to act as an infinite sink with constant solution properties. As a result, the protein concentration on the solution side is increased. Spikes over 500 kPa are observed immediately after reducing the chamber volume. When the pressure stabilized again, the pressure and plunger height were again recorded, and the process was repeated until the desired concentration-pressure curve was obtained.

After completion of the series of sample measurements, the device was dismantled, and a sample of the final concentrated solute was obtained and weighed. Protein concentration at the end of each series was determined using a spectrophotometer (Cary 50 Bio UV-VIS, Agilent, Santa Clara, CA, USA) at 280 nm for diluted samples (sample size about 0.1 g but with an accuracy of ± 0.001g) at a 350:1 ratio. The mass of the initial load and final concentration were used to calculate the concentrations of the subsequent sample sizes based on the changing volume. An

example calculation is illustrated in the supplement (S2. Example Concentration Calculations). A representative calibration curve is shown in the supplement (Figure S5).

RESULTS

Osmotic pressure profiles

To determine hydration and ion binding, the critical osmotic pressure concentration profile is required for protein concentrations near saturation. For this study, the concentration range focused in this region of interest beginning at approximately 200 – 300 g L^{-1}. Regression hydration and ion binding parameters extracted from this upper part of the osmotic pressure profile can potentially have significant error[23], especially given the error observed in this region by previous investigators.[15,28] Therefore, six trials were performed at elevated concentrations as a proof of concept. Figure 3 provides a representative curve of the pressure profile during operation. Pressure readings were found to reach equilibrium in less than one hour, albeit, since changes in volume were performed manually, the time between changes were arbitrary and sometimes up to 30 h. Nevertheless, the results illustrated that the pressure during these large intervals remained relatively constant demonstrating less than a 1% variation in pressure for a 30 h period where the volume was held constant (Figure 3). The pressure profiles for each case are shown in the supplement (S3. Raw Data. Figures S6-S12). The corresponding solute chamber volume measurements are shown in the supplement (S4. Chamber Heights for Concentration Steps, Table S1).

The osmotic pressure for BSA solutions, in 0.15M NaCl at pH 7.4, 25°C, are shown in Table 1. Concentrated osmotic pressure for BSA has been previously studied[22] and literature data in the observed concentration range was used for a comparison between the concentrating osmometer and a conventional osmometer. Figure 4 shows a plot of the results from the six trials

and the results from the literature. Example calculations are in the supplement (S5. Example Calculations).

Table 1. Osmotic Pressure of BSA in 0.15M NaCl, pH 7.4, 25°C

Literature*		Trial 1		Trial 2		Trial 3		Trial 4		Trial 5		Trial 6	
[BSA] (g L^{-1} Soln)	Osmotic Pressure (kPa)	[BSA] (g L^{-1} Soln)	Osmotic Pressure (kPa)	[BSA] (g L^{-1} Soln)	Osmotic Pressure (kPa)	[BSA] (g L^{-1} Soln)	Osmotic Pressure (kPa)	[BSA] (g L^{-1} Soln)	Osmotic Pressure (kPa)	[BSA] (g L^{-1} Soln)	Osmotic Pressure (kPa)	[BSA] (g L^{-1} Soln)	Osmotic Pressure (kPa)
84	6.4	309	120.4	212	57.0	178	49.1	241	54.7	304	108.2	324	143.3
91	7.9	314	128.3	219	69.1	189	53.0	245	60.5	311	120.7	328	170.8
211	44.3	323	139.7	261	93.6	195	56.7	247	67.3	316	115.8	333	165.9
211	44.5	331	149.7	297	113.3	213	61.2	250	72.9	323	128.9	335	189.1
289	112.5	335	159.3	301	131.9	216	70.1	254	77.3	325	142.0	339	175.6
325	132.8			322	168.1	242	81.5	258	82.5	331	153.1	345	193.3
325	132.8			322	184.6	245	91.9	265	91.9	333	174.4	350	214.0
354	189.7			327	206.3	261	102.5	269	97.9	340	188.9	353	187.6
357	218.4			330	212.5	268	106.7	285	102.3	344	206.8	356	218.1
				335	235.9	276	113.0	292	107.8	357	216.5		
				341	239.1	291	115.2	292	114.8	362	215.8		
				344	258.0	297	127.9	293	122.4	360	224.1		
				338	296.5	304	137.9	307	135.1	364	233.0		
				354	302.9	341	145.7	311	142.4	367	244.1		
				353	330.2	345	158.7	308	151.6	372	259.2		
						350	184.5	321	160.4				
						368	196.9	323	167.0				
						368	205.2						
						373	212.1						

*Data from Vilker et al.[22]

Calculation of hydration, ν_{12}, and ion binding parameters, ν_{32}

The osmotic pressure profiles for each trial were used to regress (TableCurve 2D, Systat Software, San Jose, CA) the best fit values of the hydration, ν_{12}, and ion binding parameters, ν_{32}, of the FSB model (Eqn. (2)). The best fit curves for the FSB model for the aggregate combination of the data and the literature values are shown in Figure 4. Table 2 shows the resulting hydration and ion binding parameters for each the trials and for the overall combination of all six trials.

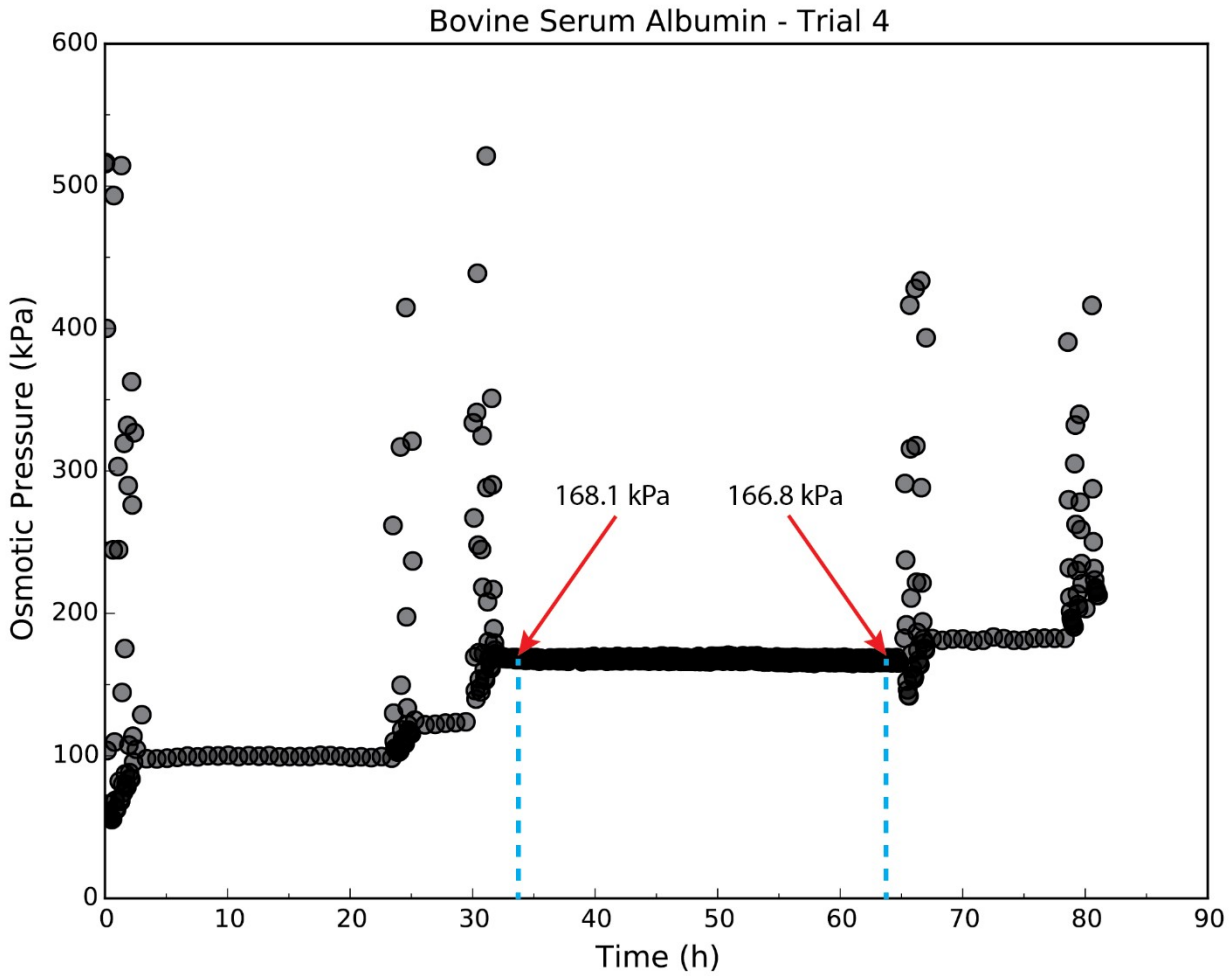

Figure 3: Representative pressure curve for obtaining the osmotic pressure profile for Trial 4. The high pressure surges represent the point at which the volume was reduced to begin the next sample. The dashed lines illustrate that between a time interval of 30 h, the pressure readings remained relatively constant with only a 0.8% loss in pressure between measurements. The actual time required between measurements to reach steady-state was determined to be approximately one hour.

With increased concentration, the osmotic pressure changes rapidly and may alter the membrane integrity of conventional membrane osmometers. As mentioned above, the concentrating osmometer presented here demonstrated sustained pressure readings for periods on the order of one day. This observation allays concerns of device leakage and offers further reliability in the results, particularly at high concentrations.

Table 2. Regressed Ion Binding and Hydration Parameters from Osmotic Pressure Data

0.15 M NaCl, pH 7.4, 25°C	Concentration ($g\ L^{-1}$) [Data Points]	Hydration ($\frac{mol\ H_2O}{mol\ BSA}$) ν_{12}	Ion Binding ($\frac{mol\ Salt}{mol\ BSA}$) ν_{32}	Covariance
Literature*	84 – 357 [9]	5499 ± 557	13.05 ± 2.17	2.08×10^{-5}
Trial 1	309 – 335 [5]	5168 ± 489	11.76 ± 1.80	5.93×10^{-7}
Trial 2	212 – 353 [15]	6212 ± 387	14.77 ± 1.70	1.80×10^{-5}
Trial 3	178 – 373 [19]	3386 ± 478	4.99 ± 1.82	1.80×10^{-5}
Trial 4	241 – 323 [17]	6135 ± 380	14.49 ± 1.36	3.65×10^{-6}
Trial 5	304 – 372 [15]	5364 ± 372	12.41 ± 1.53	5.66×10^{-6}
Trial 6	324 – 356 [9]	4762 ± 1571	9.86 ± 6.26	2.46×10^{-4}
Aggregated Trials	178 – 373 [80]	4687 ± 564	9.47 ± 2.24	4.45×10^{-5}

*Data from Vilker et al.[22]

DISCUSSION

Error analysis of the osmotic pressure profile at high concentrations

As seen in Figure 4, with the exception of Trial 2, there is an error of 18% in the osmotic pressure results for the highest value. This level of error is consistent with what was observed previously by Kappos and Pauly (1966). We have previously shown that the sensitivity of osmotic pressure increases significantly near saturation conditions.[23]

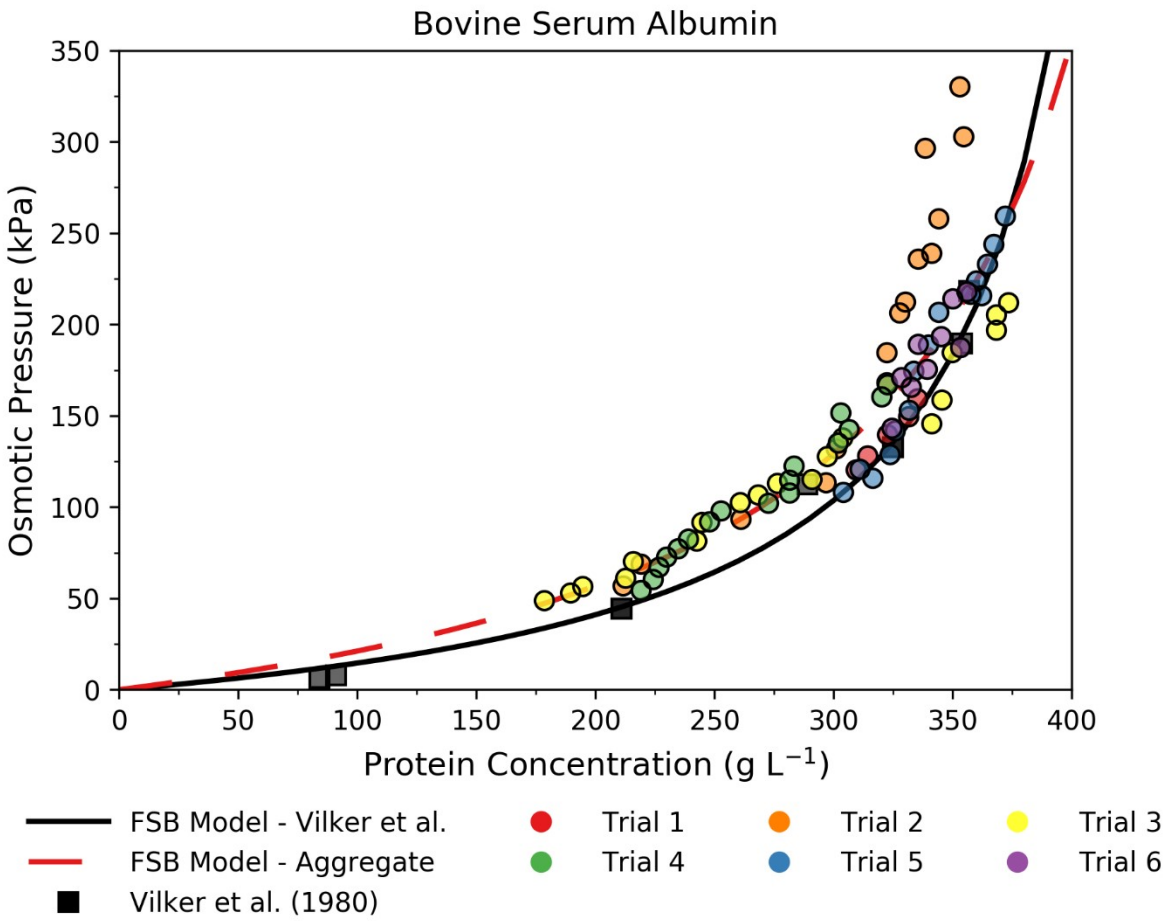

Figure 4: Osmotic pressure data, from a concentrating osmometer, for BSA in 0.15M NaCl at pH 7.4, 25°C, and values taken from the Vilker et al. (1981)[22]. Overall, the pressure measurements made with the concentrating osmometer are in excellent agreement with the results from the literature, albeit, the latter values for Trial 2 appear high.

Nearly all of the results produced an osmotic pressure for specific concentrations of BSA that were higher than that presented by Vilker et al. (albeit, the results from Trial 2 are notably higher). The observed slightly higher data values may be due to modest changes in ionic strength from the work of Vilker. Because the solvent chamber was on the order of the size of the solution chamber, Vilker, used aliquots of 0.1 N NaOH or 0.1 N HCl to adjust pH. He did not measure the change in ionic strength but estimated it to be as much as ± 0.03 M.[15]

The error related to the height and absorbance measurements in our work are calculated to be less than ± 1% and ± 0.5%, respectively, with pressure transducer error documented at less than

± 2 kPa. The large deviation in the osmotic pressure from Trial 2 is likely coupled to an error in solution preparation.

Advantages and disadvantages of concentrating membrane osmometer over conventional devices

The concentrating osmometer has a number of advantages over conventional devices when generating osmotic pressure profiles. Perhaps the primary advantages are; 1) the preparation time is reduced, 2) the operation time is reduced, 3) the associated labor is reduced and 4) a lower quantity of sample is required for the complete osmotic pressure profile. In conventional osmometers, preparation of a single osmotic pressure profile took several weeks and required a series of sample preparations and device loading. At higher concentrations, a single solution preparation could take as much as two days.[15,18]

A disadvantage is of the concentrating osmometer is that sampling error can propagate throughout the entire concentration range for the profile. Using error propagation, the variance in c_n, $\sigma_{c_n}^2$, is

$$\sigma_{c_n}^2 = \left(\frac{\sigma_{m_o}}{V_o - \sum_{j=2}^{n} \Delta V_j}\right)^2 + \left(\frac{m_o}{\left(V_o - \sum_{j=2}^{n} \Delta V_j\right)^2}\right)^2 \sigma_{V_o}^2 + \sum_{i=1}^{n} \left(\frac{m_o}{\left(V_o - \sum_{j=2}^{n} \Delta V_j\right)^2}\right)^2 \sigma_{\Delta V_i}^2, \quad (3)$$

where σ_{m_o} is the error in the measurement of the initial mass, $\sigma_{V_o}^2$ is the variance in the initial volume and $\sigma_{\Delta V_i}^2$ is the variance in the i^{th} volume change. One can see that as n increases, the error in c_n increases significantly. With fixed $\sigma_{\Delta V_i}^2$ the error propagates at a minimum rate of $\sqrt{n-1}\,\sigma_{\Delta V_i}$. Even with excellent sample preparation, a dramatic increase in error is expected at high concentrations, particularly as $V_o - \sum_{j=2}^{n} \Delta V_j \to 0$. Thus, researchers should be mindful of the potential error in using the concentrating osmometer.

CONCLUSION

Here, a concentrating osmometer for determining an osmotic pressure profile for a colloid solution from a single sample was developed and tested. The practical issues and applications were discussed. The concentrating osmometer was tested for a BSA solution in 0.15 M NaCl at pH 7.4. There was good agreement between the osmotic pressure profile and the regressed hydration and ion binding values between this study and the literature.

The concentrating osmometer can substantially reduce the required quantity of protein used to obtain the osmotic pressure profile and can significantly reduce the time required to obtain a complete osmotic pressure profile. One should be aware of the propagation of error from the initial sample measurements when evaluating the results. Although the study often used large variations between volume changes, the results show that the system reaches steady-state within one hour. Thus, an osmotic pressure profile for a region of interest for highly colloid solutions can be obtained on the order of one day with substantially reduced preparation error. Since the sample size required to generate the osmotic pressure profile is substantially reduced, gram quantities of the protein are no longer required.

SUPPLEMENT MATERIAL

The supplement contains:

S1. Design Specifications
S2. Absorbance Calibration
S3. Raw Data
S4. Chamber Heights for Concentration Steps
S5. Example Concentration Calculations (Trial 4)

ACKNOWLEDGEMENTS

This device and its applications are described in a provisional patent application (US20150141950A1) submitted by the authors and the University of California, Riverside. There is no commercial support at this time. The authors have no conflicts of interest to report.

This work was funded by an endowment from Jacques S. Yeager, Sr. Partial support for Devin McBride was provided by the NSF IGERT Video Bioinformatics Fellowship Grant (DGE 0903667).

REFERENCES

1. Hoff, J. H. van't. *Etudes de Dynamique Chimique*. (Frederik Muller & Co., 1884).
2. Van't Hoff, J. The function of osmotic pressure in the analogy between solutions and gases. *Proc. Phys. Soc. London* (1886). doi:10.1088/1478-7814/9/1/344
3. Hitchcock, D. I. Osmotic pressure and molecular weight. *J. Chem. Educ.* **28,** 478 (1951).
4. Peterson, S. The molecular weight of a protein: A student determination of osmotic pressure. *J. Chem. Educ.* **28,** 486 (1951).
5. Candlish, J. K. Simple Construction to Determine Protein Molecular Weights by Osmotic Pressure Method. *J. Chem. Educ.* **45,** 93- (1968).
6. Fullerton, G. D., Zimmerman, R. J., Kanal, K. M., Floyd, L. J. & Cameron, I. L. Method to Improve the Accuracy of Membrane Osmometry Measures of Protein Molecular-Weight. *J. Biochem. Biophys. Methods* **26,** 299–307 (1993).
7. Lewis, G. N. The Osmotic Pressure of Concentrated Solutions, and the Laws of the Perfect Solution. *J. Am. Chem. Soc.* **30,** 668–683 (1908).
8. Orofino, T. A. & Flory, P. J. Relationship of the second virial coefficient to polymer chain dimensions and interaction parameters. *J. Chem. Phys.* (1957). doi:10.1063/1.1743472
9. Stigter, D. Interactions in aqueous solutions. II. Osmotic pressure and osmotic coefficient of sucrose and glucose solutions. *J. Phys. Chem.* (1960). doi:10.1021/j100830a028
10. Neal, B. L., Asthagiri, D. & Lenhoff, A. M. Molecular origins of osmotic second virial coefficients of proteins. *Biophys. J.* (1998). doi:10.1016/S0006-3495(98)77691-X
11. Neal, B. L., Asthagiri, D., Velev, O. D., Lenhoff, A. M. & Kaler, E. W. Why is the osmotic second virial coefficient related to protein crystallization? *J. Cryst. Growth* (1999). doi:10.1016/S0022-0248(98)00855-0
12. Guo, B. *et al.* Correlation of second virial coefficients and solubilities useful in protein

crystal growth. *J. Cryst. Growth* (1999). doi:10.1016/S0022-0248(98)00842-2

13. Ruppert, S., Sandler, S. I. & Lenhoff, a M. Correlation between the Osmotic Second Virial Coefficient and the Solubility of Proteins - Ruppert - 2008 - Biotechnology Progress - Wiley Online Library. *Biotechnol. Prog.* (2001). doi:10.1021/bp0001314
14. Binabaji, E., Rao, S. & Zydney, A. L. The osmotic pressure of highly concentrated monoclonal antibody solutions: Effect of solution conditions. *Biotech Bioeng* (2013).
15. Vilker, V. L. Ph. D. Dissertation. The ultrafiltration of biological macromolecules. (Massachusetts Institute of Technology. Dept. of Chemical Engineering., 1975).
16. Wu, J. Z. & Prausnitz, J. M. Osmotic pressures of aqueous bovine serum albumin solutions at high ionic strength. *Fluid Phase Equilib.* **155,** 139–154 (1999).
17. Yousef, M. A. A., Datta, R. & Rodgers, V. G. J. Free-solvent model of osmotic pressure revisited: Application to concentrated IgG solution under physiological conditions. *J. Colloid Interface Sci.* **197,** 108–118 (1998).
18. Yousef, M. A. A., Datta, R. & Rodgers, V. G. J. Confirmation of free solvent model assumptions in predicting the osmotic pressure of concentrated globular proteins. *J. Colloid Interface Sci.* **243,** 321–325 (2001).
19. Yousef, M. A., Datta, R. & Rodgers, V. G. J. Monolayer hydration governs nonideality in osmotic pressure of protein solutions. *AIChE J.* **48,** (2002).
20. Yousef, M. A., Datta, R. & Rodgers, V. G. J. Model of osmotic pressure for high concentrated binary protein solutions. *AIChE J.* **48,** (2002).
21. Hale, C. S. *et al.* Interrogating the Osmotic Pressure of Self-Crowded Bovine Serum Albumin Solutions: Implications of Specific Monovalent Anion Effects Relative to the Hofmeister Series. *J. Phys. Chem. B* **122,** 8037–8046 (2018).

22. Vilker, V. L., Colton, C. K. & Smith, K. A. The osmotic pressure of concentrated protein solutions: Effect of concentration and ph in saline solutions of bovine serum albumin. *J. Colloid Interface Sci.* **79,** 548–566 (1981).

23. Yousef, M. A. A., Datta, R. & Rodgers, V. G. J. Understanding nonidealities of the osmotic pressure of concentrated bovine serum albumin. *J. Colloid Interface Sci.* **207,** 273–282 (1998).

24. McBride, D. W. & Rodgers, V. G. J. Obtaining protein solvent accessible surface area when structural data is unavailable using osmotic pressure. *AIChE J.* **58,** 1012–1017 (2012).

25. McBride, D. W. & Rodgers, V. G. J. Interpretation of negative second virial coefficients from non-attractive protein solution osmotic pressure data: An alternate perspective. *Biophys. Chem.* **184,** 79–86 (2013).

26. McBride, D. W. & Rodgers, V. G. J. Predicting the Activity Coefficients of Free-Solvent for Concentrated Globular Protein Solutions Using Independently Determined Physical Parameters. *PLoS One* **8,** (2013).

27. McBride, D. W. & Rodgers, V. G. J. A generalized free-solvent model for the osmotic pressure of multi-component solutions containing protein-protein interactions. *Math. Biosci.* **253,** 72–87 (2014).

28. Kappos, A. D. & Pauly, H. [Osmotic measurements on high concentrated solutions of bovine serum albumin]. *Biophysik* **3,** 131–9 (1966).

29. Scatchard, G., Batchelder, A. C., Brown, A. & Zosa, M. Preparation and Properties of Serum and Plasma Proteins. VII. Osmotic Equilibria in Concentrated Solutions of Serum Albumin1,2. *J. Am. Chem. Soc.* **68,** 2610–2612 (1946).

30. Zimm, B. H. & Myerson, I. A Convenient Small Osmometer. *J. Am. Chem. Soc.* **68,** 911–912 (1946).

31. Bruss, D. B. & Stross, F. H. A Small-Volume High-Speed Osmometer. *Anal. Chem.* **32,** 1456–1458 (1960).

32. Rolfson, F. B. & Coll, H. Automatic Osmometer for Determination of Number Average Molecular Weights of Polymers. *Anal. Chem.* (1964). doi:10.1021/ac60210a055

33. Myrenne, K.-D. S. High-speed microvolume membrane osmometry. U.S. Patent No. 3,661,011. 9 May 1972.

34. Steudle, E. & Stumpf, B. Process and apparatus for the determination of the concentration of a substance dissolved in a solvent by means of an osmometer. U.S. Patent No. 5,005,403. 9 Apr. 1991.

35. Amos, D., Markels, J., Lynn, S. & Radke, C. Osmotic pressure and interparticle interactions in ionic micellar surfactant solutions. *J. Phys. Chem. B* (1998). doi:10.1021/jp9805407

36. Boris, D. C. Method for measuring changes in osmotic pressure. U.S. Patent No. 6,267,003. 31 Jul. 2001.

37. Wang, Y. & Rodgers, V. G. J. Free-solvent model shows osmotic pressure is the dominant factor in limiting flux during protein ultrafiltration. *J. Memb. Sci.* **320,** 335–343 (2008).

38. Wang, Y. H. & Rodgers, V. G. J. Determining Fouling-Independent Component of Critical Flux in Protein Ultrafiltration Using the Free-Solvent-Based (FSB) Model. *Aiche J.* **56,** 2756–2759 (2010).

Detailed Design Specification, Calibration Curve and Raw Osmotic Pressure Data

S1. Design Specifications

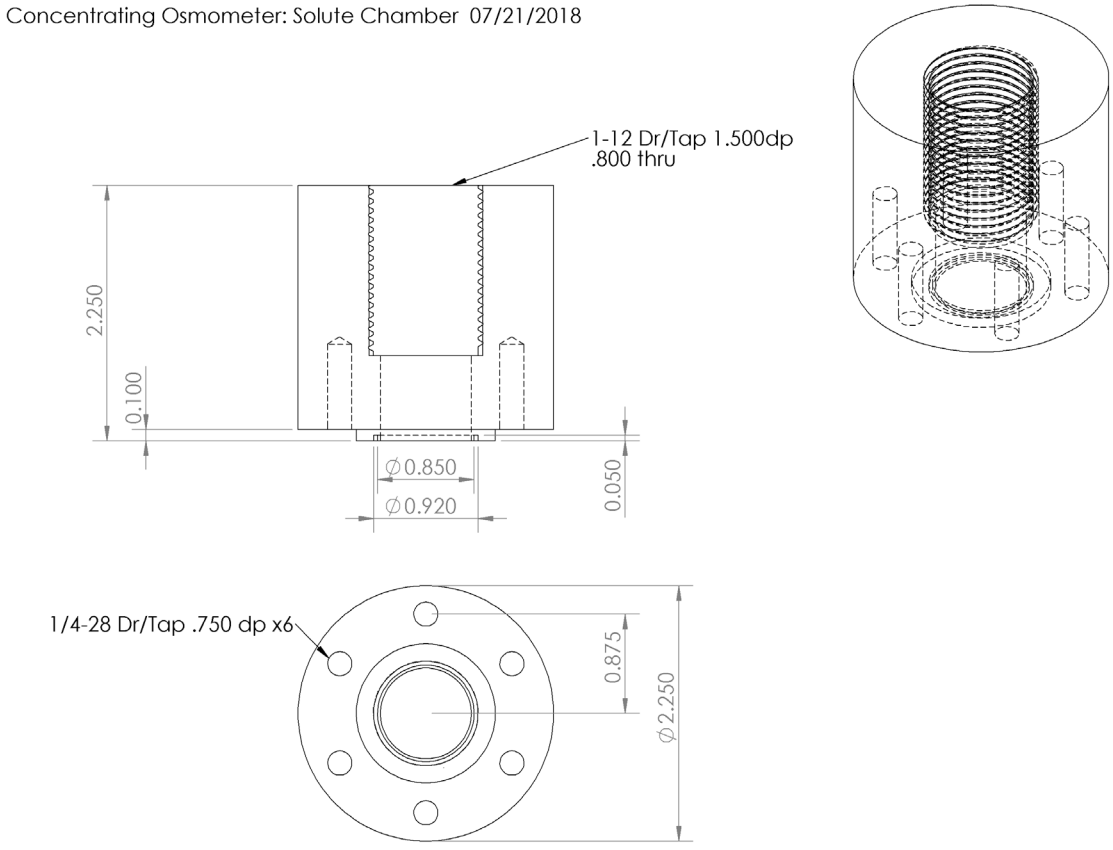

Figure S1: Detail design specifications for the solute chamber.

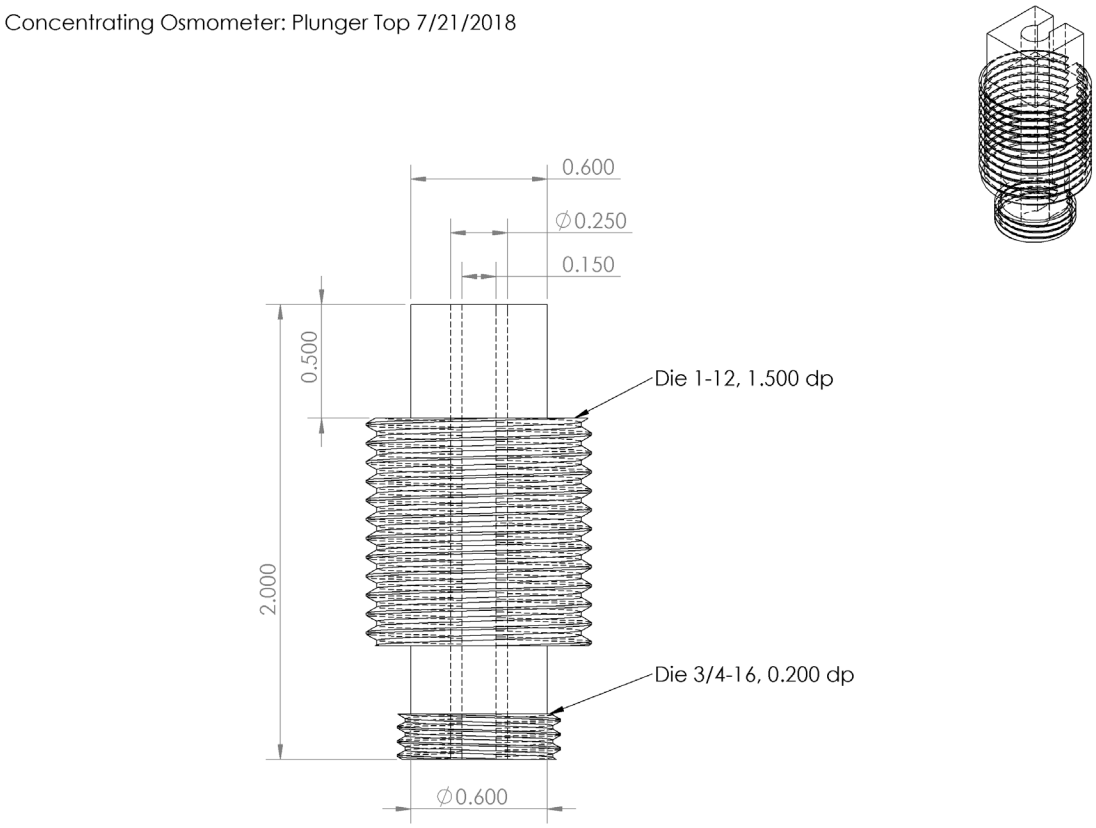

Figure S2: Detailed design specifications for the device plunger top.

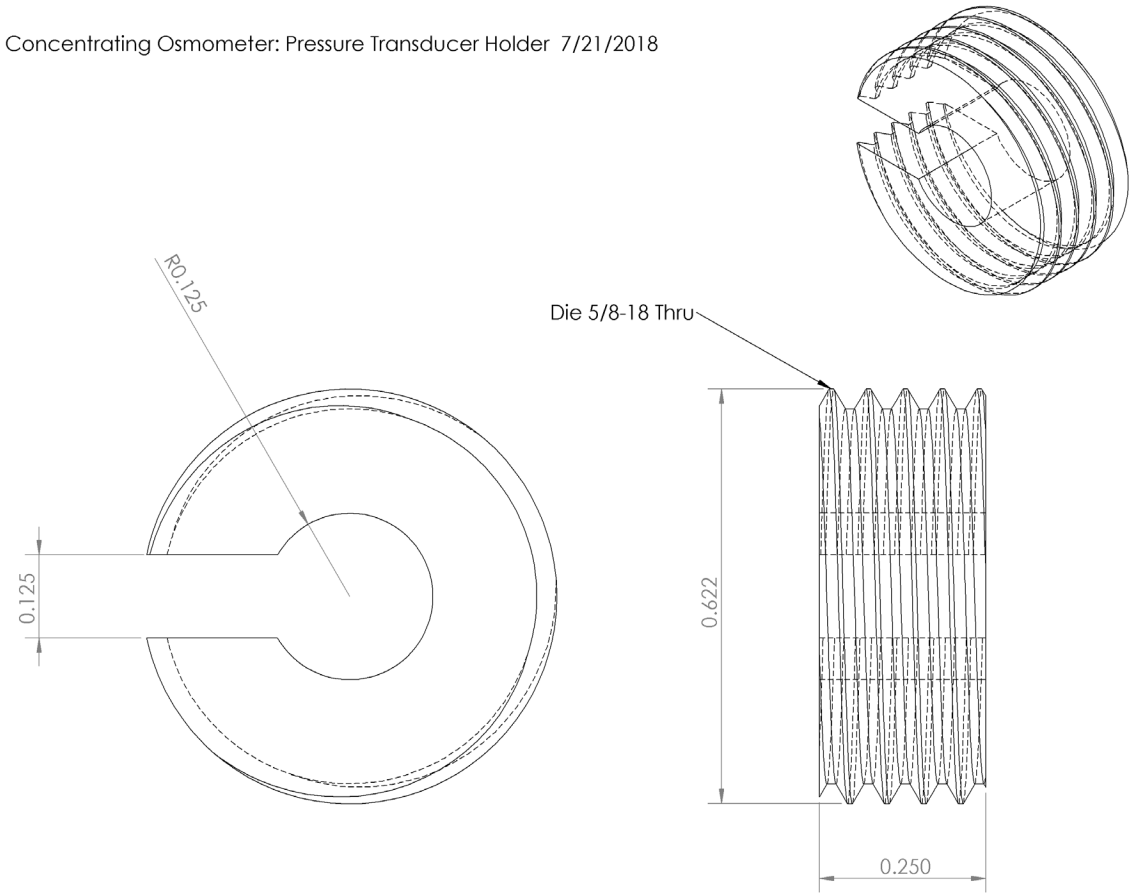

Figure S3: Detailed design specifications for the device plunger holder.

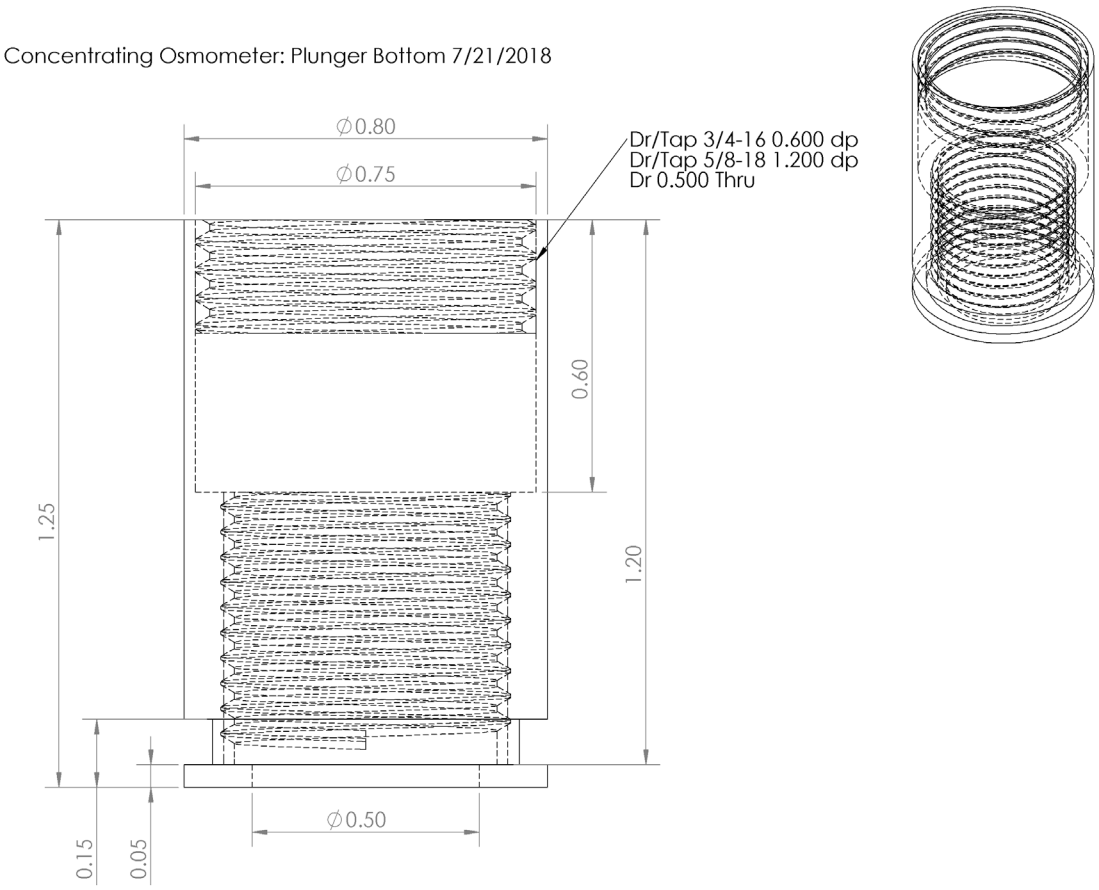

Figure S4: Detailed design specifications for the device plunger bottom.

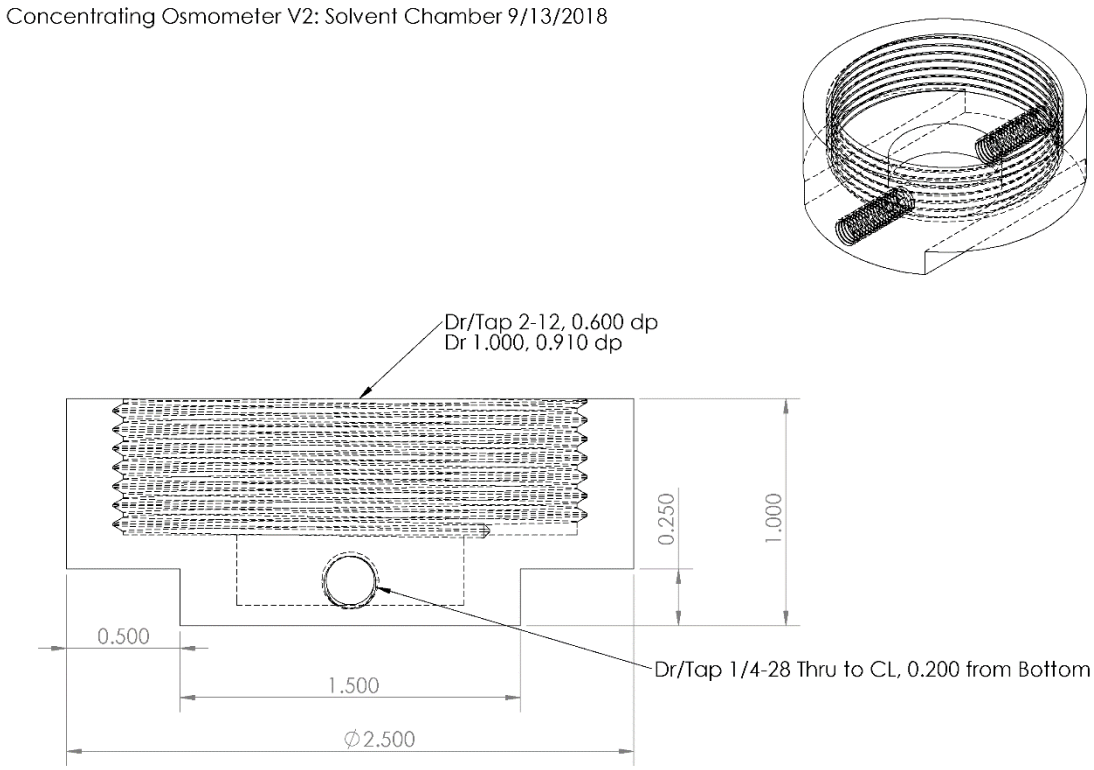

Figure S5: Detailed design specifications for the solvent chamber.

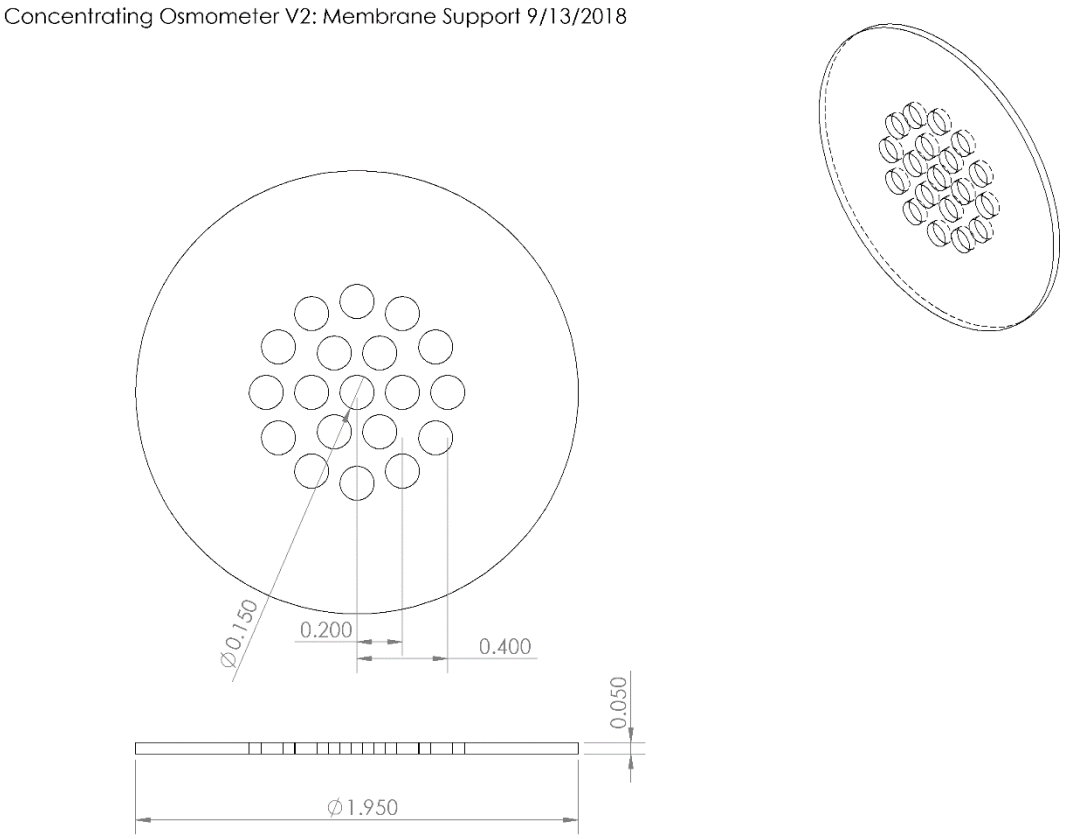

Figure S6: Detailed design specifications for the membrane support.

S2. Absorbance Calibration

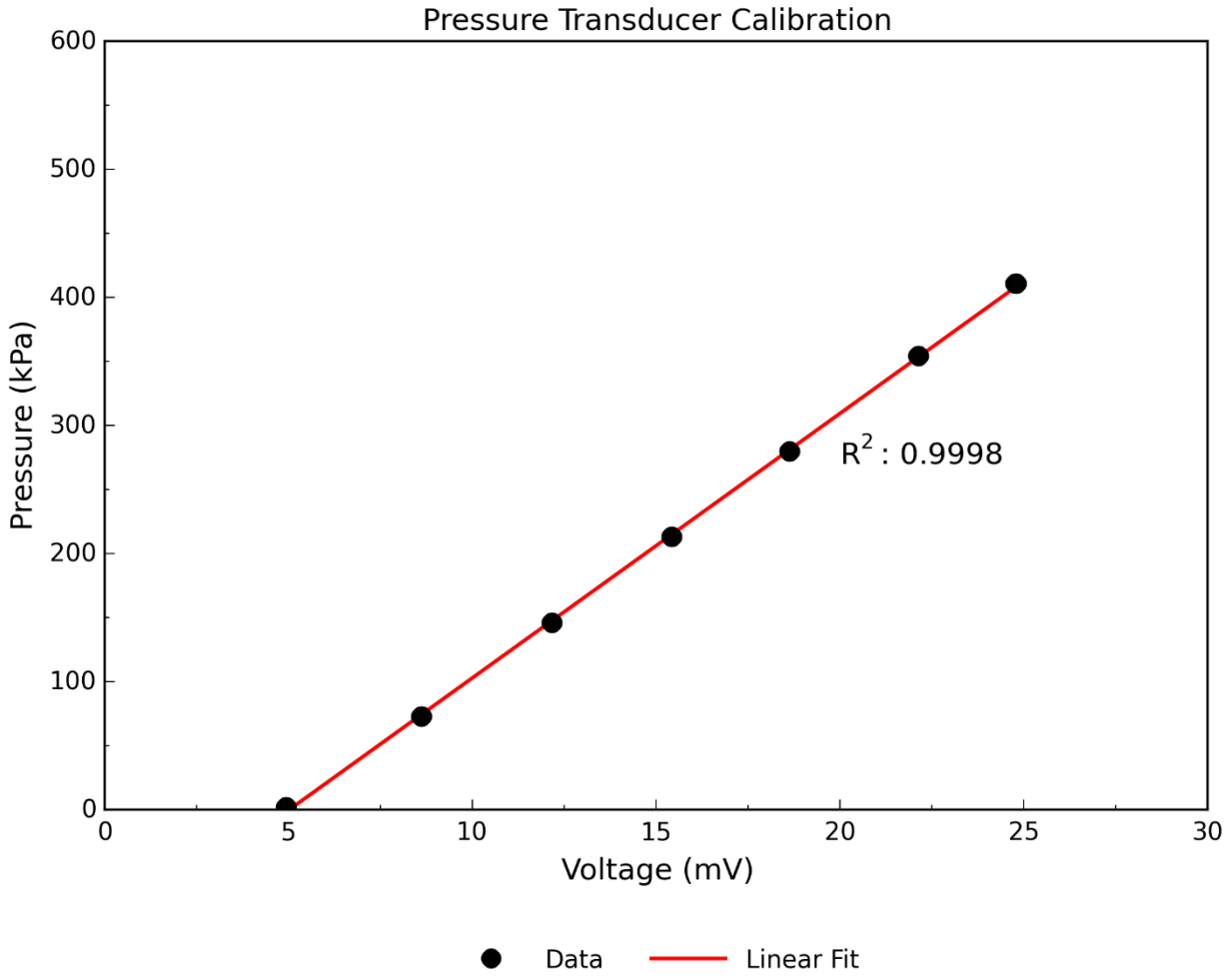

Figure S7: Representative calibration curve for bovine serum albumin solutions used in the trials. The sample from the device was diluted by a 350:1 ratio.

S3. Raw Data

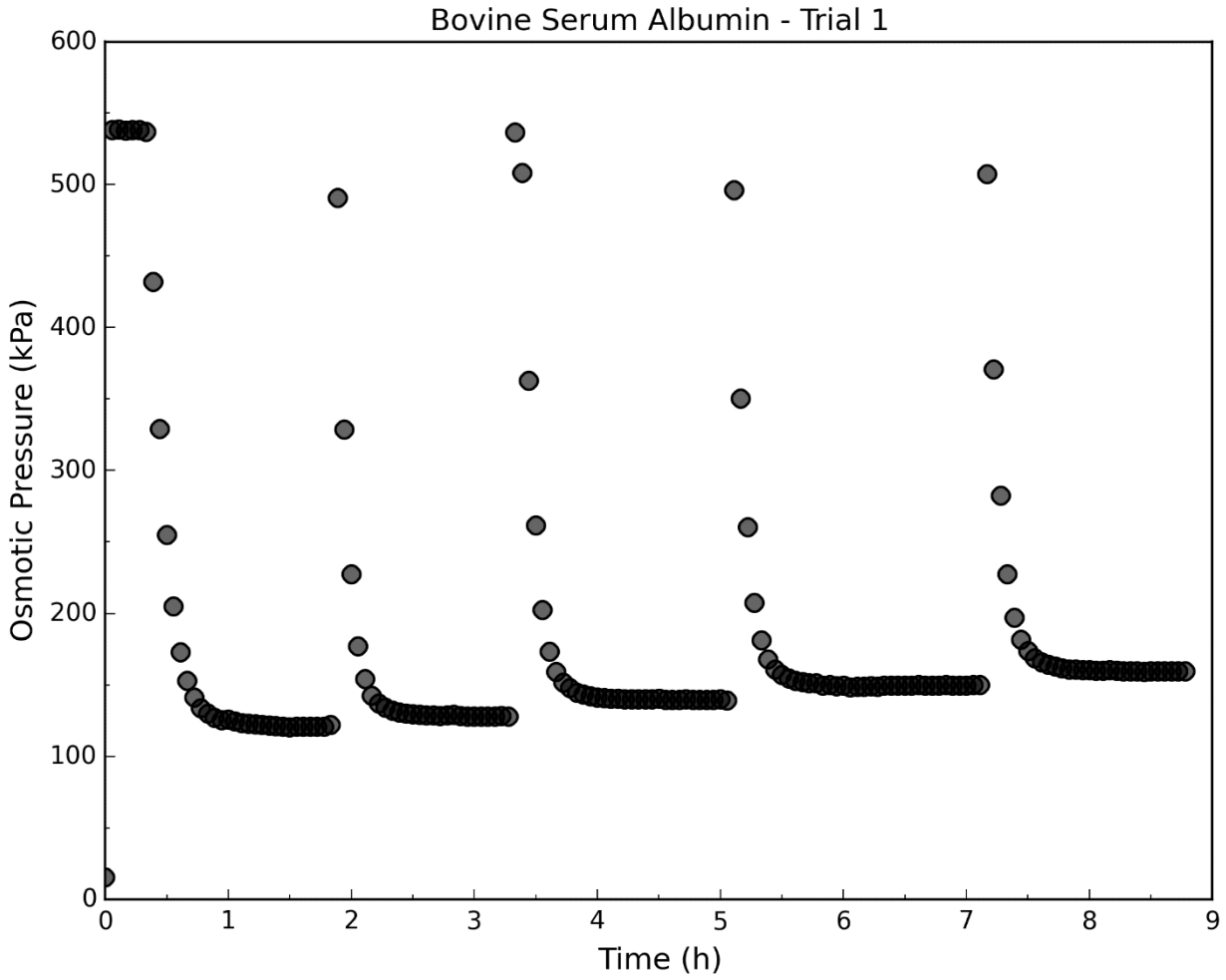

Figure S8: Pressure profile obtained from Trial 1. The high pressure surges represent the point at which the volume was reduced to begin the next sample. As can be seen, the pressure measurement settles down rapidly and reaches a steady value within one hour.

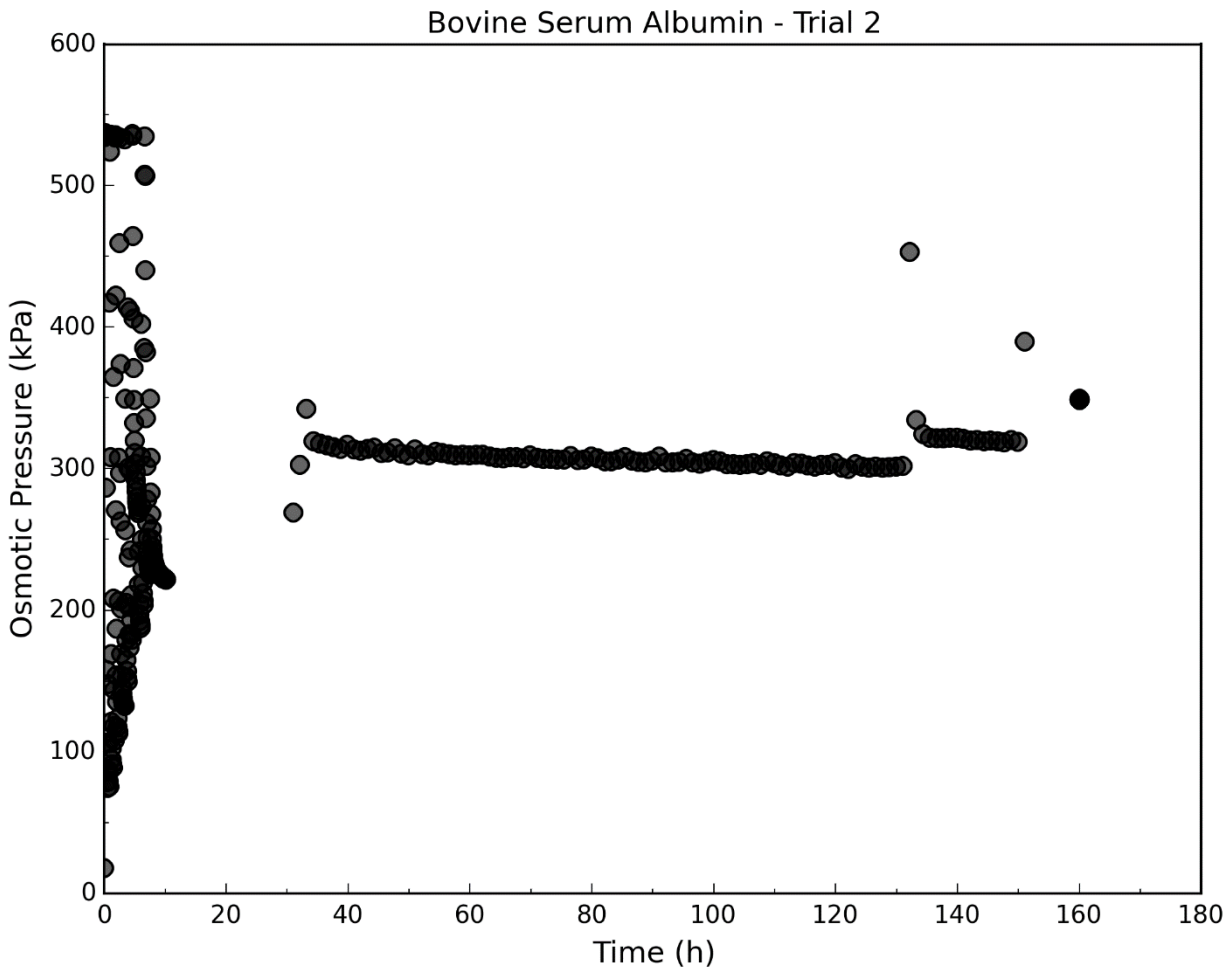

Figure S9: Pressure profile obtained from Trial 2. The high pressure surges represent the point at which the volume was reduced to begin the next sample. The time between the latter samples was on the order of 100 h and the sample pressure remained relatively stable.

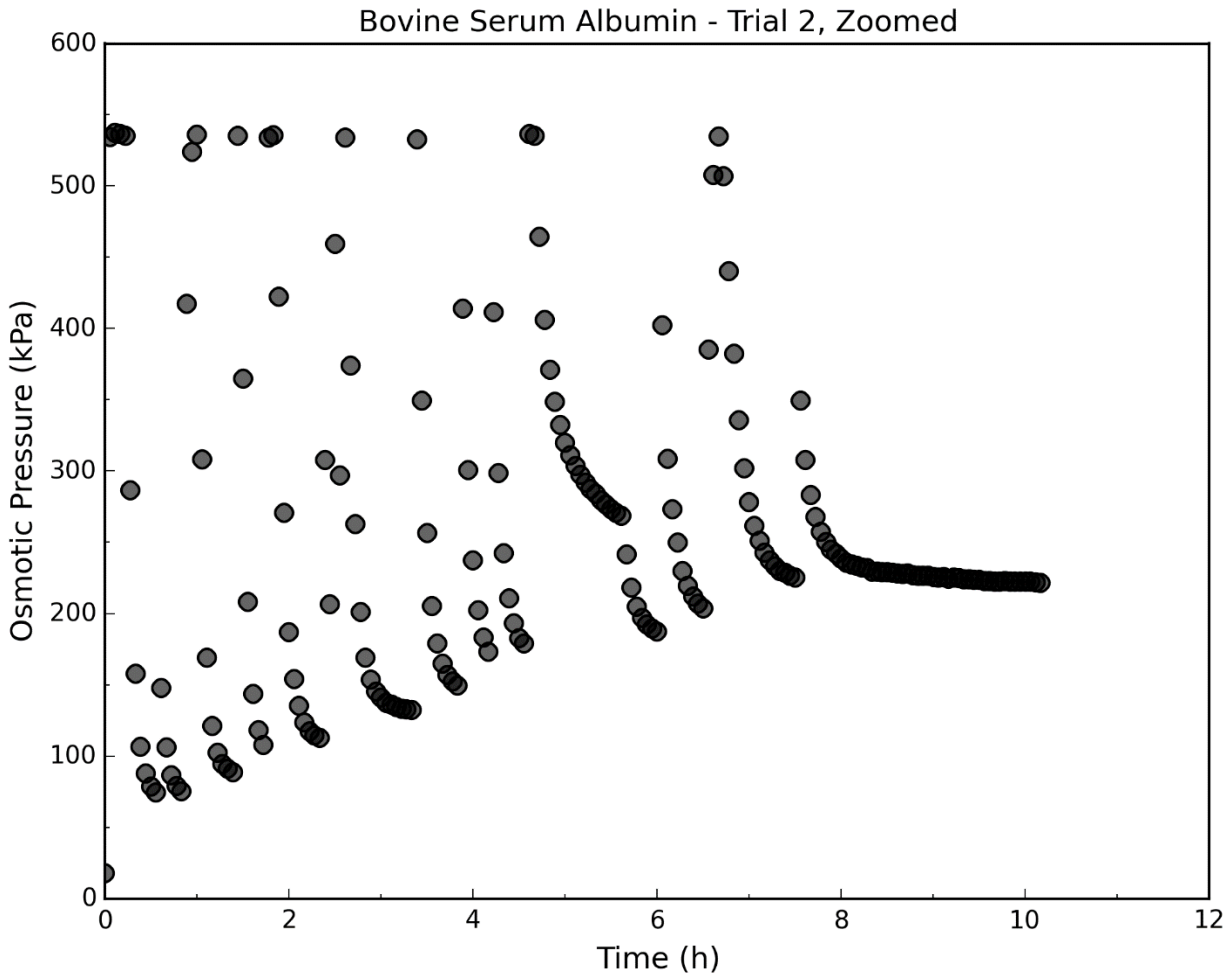

Figure S10: Pressure profile obtained from Trial 2 for the first 12 h only. The high pressure surges represent the point at which the volume was reduced to begin the next sample.

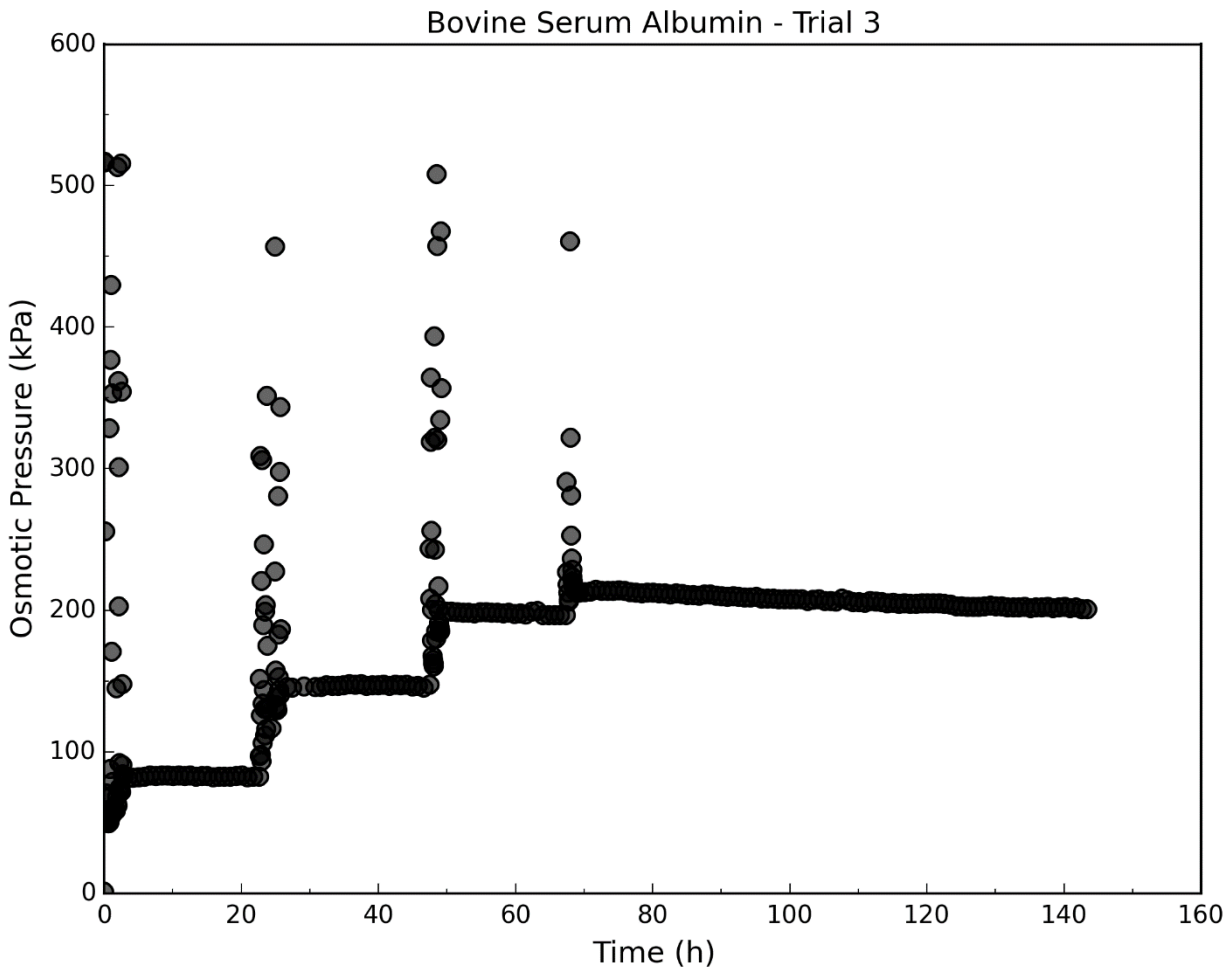

Figure S11: Pressure profile obtained from Trial 3. The high pressure surges represent the point at which the volume was reduced to begin the next sample. The time between the samples were on the order of 20 h for the initial cases and approximately 70 h between the last two points.

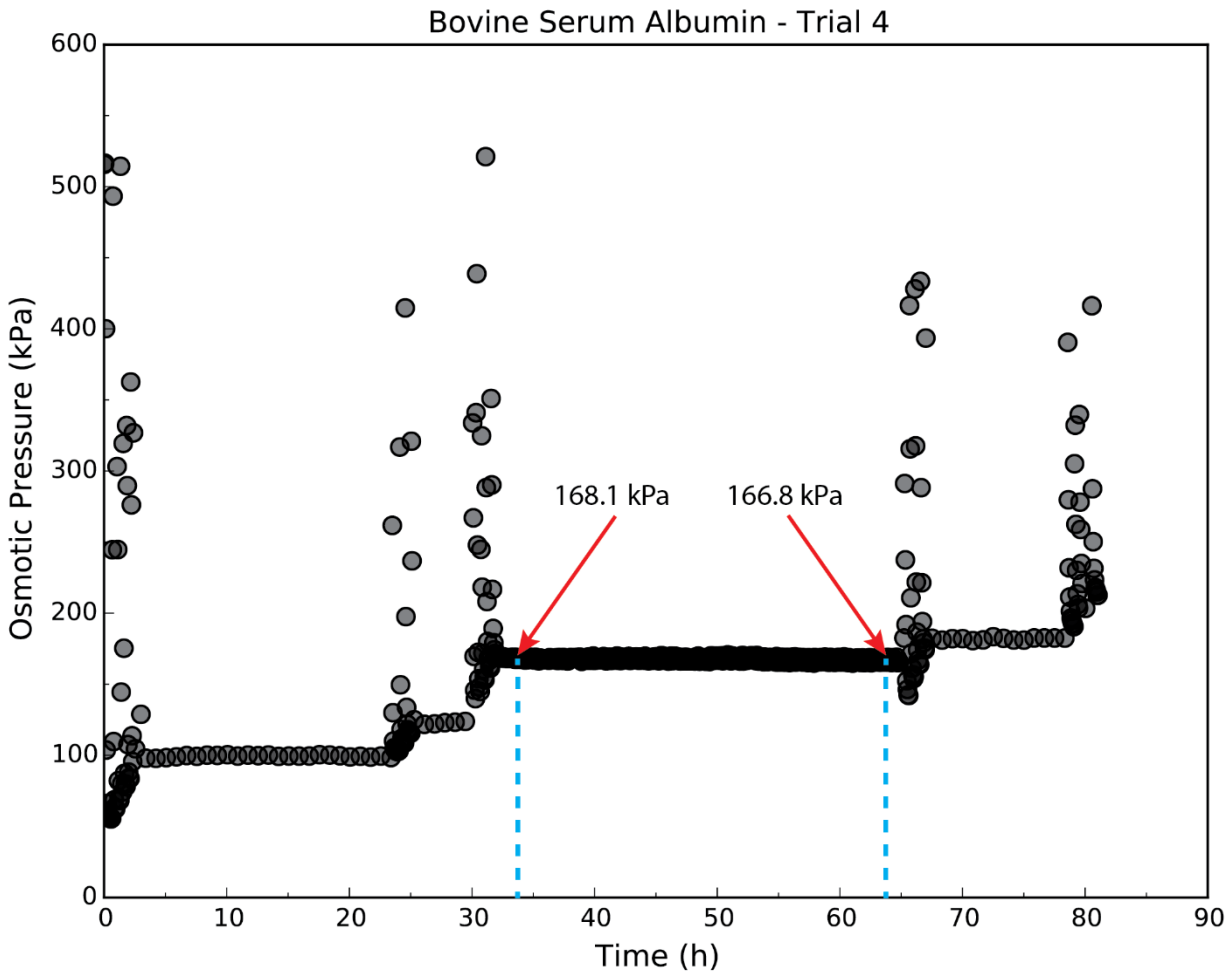

Figure S12: Pressure profile obtained from Trial 4. The high pressure surges represent the point at which the volume was reduced to begin the next sample. The dashed lines illustrate that between a time interval of 30 h, the pressure readings remained relatively constant with only a 0.8% loss in pressure between measurements.

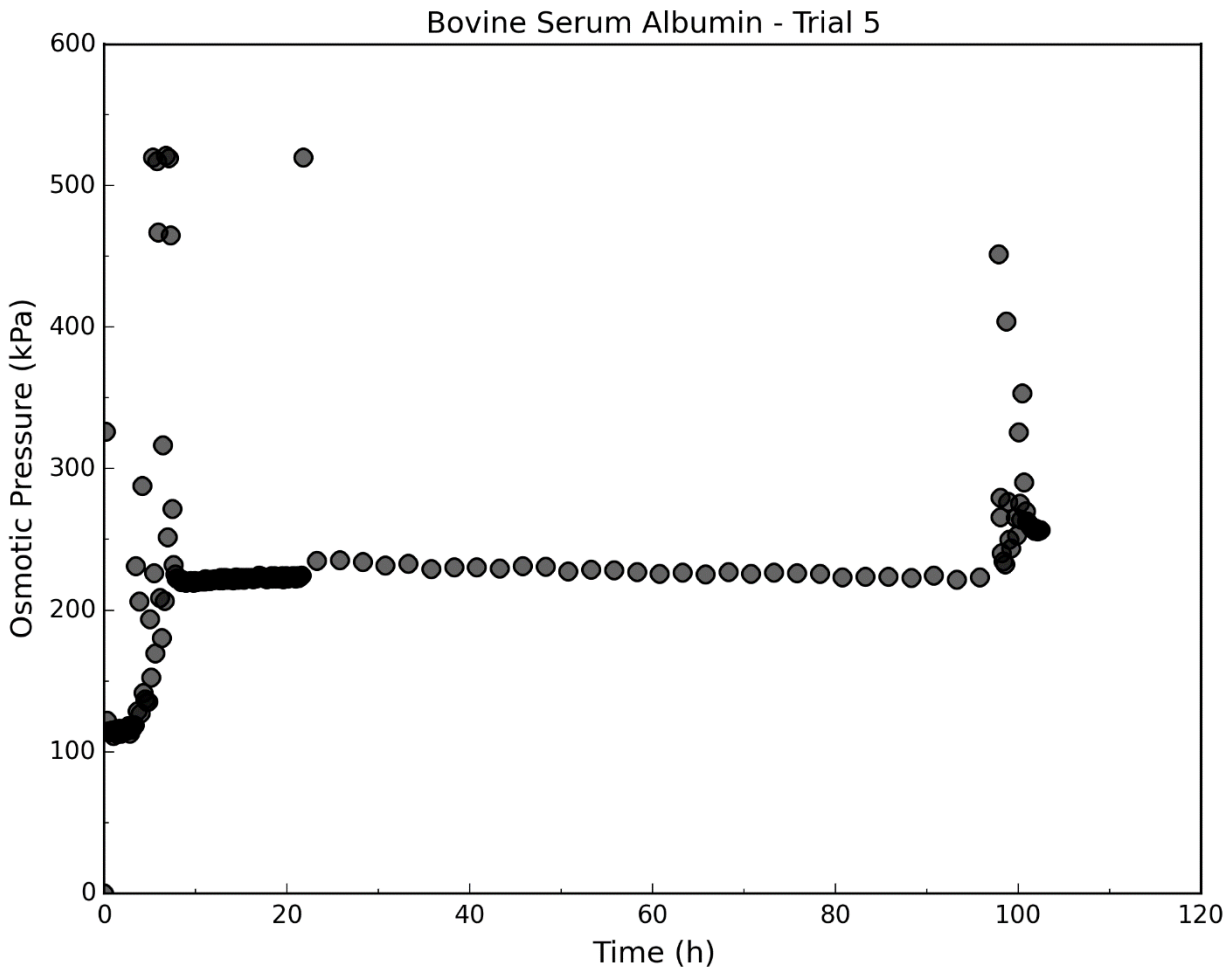

Figure S13: Pressure profile obtained from Trial 5. The high pressure surges represent the point at which the volume was reduced to begin the next sample.

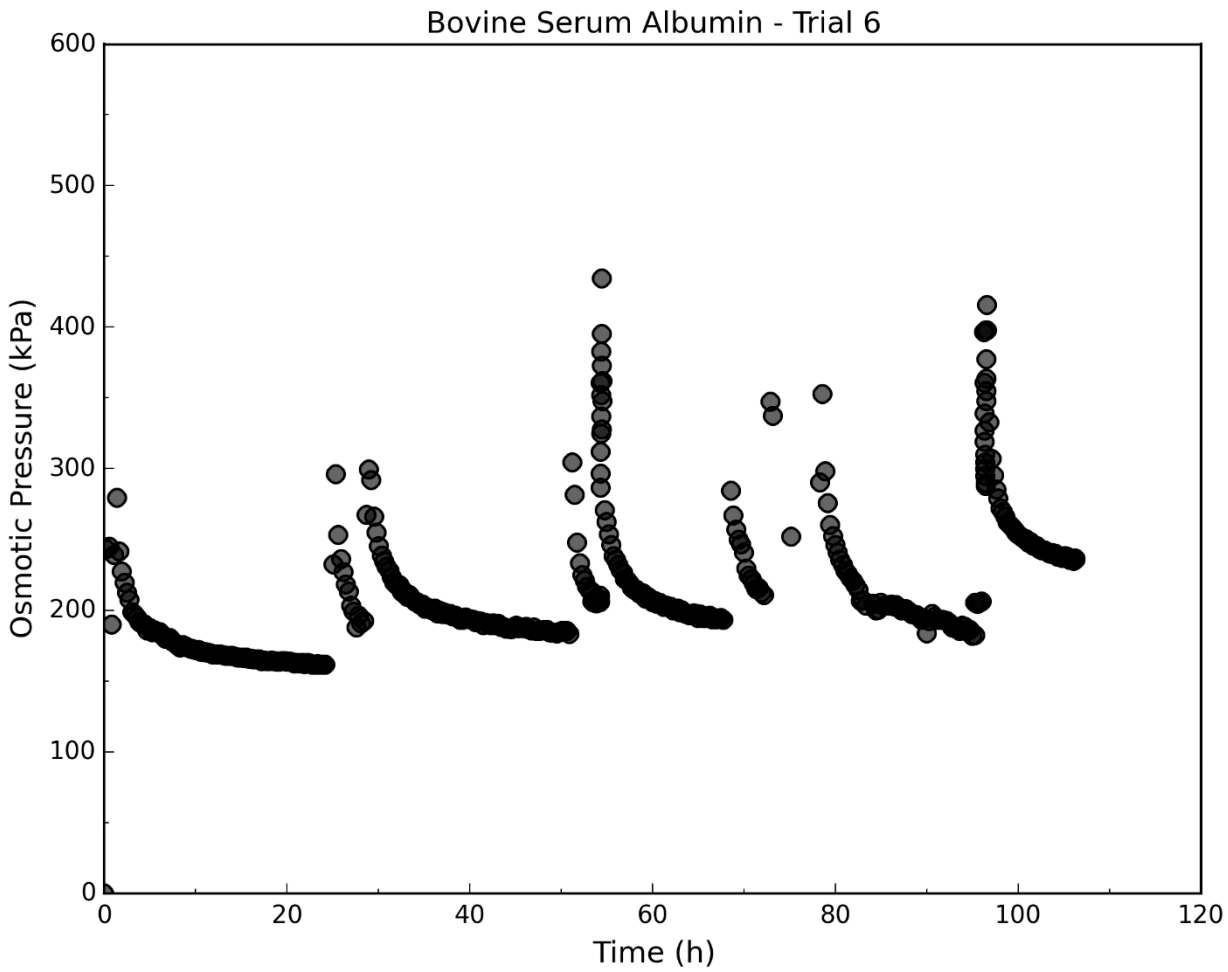

Figure S14: Pressure profile obtained from Trial 6. The high pressure surges represent the point at which the volume was reduced to begin the next sample.

S4. Chamber Heights for Concentration Steps

Table S1. Measured Solution Chamber Heights for Measurements Done During Each Trial

Trial 1		Trial 2		Trial 3		Trial 4		Trial 5		Trial 6	
Chamber Height (mm)	[BSA] (g L^{-1} Soln)	Chamber Height (mm)	[BSA] (g L^{-1} Soln)	Chamber Height (mm)	[BSA] (g L^{-1} Soln)	Chamber Height (mm)	[BSA] (g L^{-1} Soln)	Chamber Height (mm)	[BSA] (g L^{-1} Soln)	Chamber Height (mm)	[BSA] (g L^{-1} Soln)
2.997	312	2.985	220	2.197	191	2.845	246	2.845	310	2.108	324
2.921	317	2.819	227	1.969	201	2.743	250	2.743	316	2.007	328
2.794	324	2.057	268	1.867	207	2.692	252	2.667	321	1.905	333
2.667	332	1.575	301	1.562	224	2.629	255	2.565	328	1.854	335
2.616	335	1.524	305	1.511	228	2.540	259	2.540	330	1.753	339
		1.295	325	1.156	253	2.464	262	2.464	335	1.626	345
		1.295	325	1.130	255	2.311	269	2.438	337	1.524	350
		1.245	330	0.953	271	2.235	273	2.362	343	1.448	353
		1.219	332	0.876	278	1.943	288	2.311	347	1.397	356
		1.168	337	0.800	285	1.829	294	2.159	359		
		1.118	342	0.673	299	1.829	294	2.108	363		
		1.092	345	0.622	305	1.803	296	2.134	361		
		1.143	340	0.572	311	1.588	309	2.083	365		
		1.003	354	0.318	345	1.537	312	2.057	367		
		1.016	353	0.292	349	1.575	309	2.007	372		
				0.267	352	1.397	321				
				0.165	369	1.372	323				
				0.165	369						
				0.140	373						

S5. Example Concentration Calculations (Trial 4)

Trial 4 (5/15/2018)		Turns, i	Measured Height (Inches)	Chamber Height (Inches)	Vo/Vi	Calculated Concentration, Ci (g/L)	Pressure (psi)	Pressure (kPa)
Protein Solution Used (g):	**2.01**	0	**1.0095**	0.1120	1.0000	**240.7**	**7.9**	**54.7**
Protein Density (g/mL):	**1.067**	1	**1.0055**	0.1080	1.0178	**245.0**	**8.8**	**60.5**
Protein Solution Used (mL):	**1.88**	2	**1.0035**	0.1060	1.0270	**247.2**	**9.8**	**67.3**
Initial prep concentration (g/L)	201.9	3	**1.0010**	0.1035	1.0386	**250.0**	**10.6**	**72.9**
Minimum Height (Inches):	0.8975	4	**0.9975**	0.1000	1.0554	**254.1**	**11.2**	**77.3**
Total (mL, Minimum)	**0.959**	5	**0.9945**	0.0970	1.0703	**257.6**	**12.0**	**82.5**
Vo (mL, Start)	**1.881**	34	**0.9885**	0.0910	1.1012	**265.1**	**13.3**	**91.9**
		7	**0.9855**	0.0880	1.1174	**269.0**	**14.2**	**97.9**
Final Concentration, Cn (g/L):	**322.6**	8	**0.9740**	0.0765	1.1839	**285.0**	**14.8**	**102.3**
		9	**0.9695**	0.0720	1.2122	**291.8**	**15.6**	**107.8**
		10	**0.9695**	0.0720	1.2122	**291.8**	**16.7**	**114.8**
Conversion (psi to kPa):	6.8948	11	**0.9685**	0.0710	1.2187	**293.4**	**17.8**	**122.4**
		12	**0.9600**	0.0625	1.2765	**307.3**	**19.6**	**135.1**
		13	**0.9580**	0.0605	1.2910	**310.8**	**20.7**	**142.4**
		14	**0.9595**	0.0620	1.2801	**308.2**	**22.0**	**151.6**
		15	**0.9525**	0.0550	1.3324	**320.7**	**23.3**	**160.4**
Final Volume, Vn (mL, Finish)	**1.4037**	16	**0.9515**	0.0540	1.3402	**322.6**	**24.2**	**167.0**

Ci = total protein mass/ volume at the ith measurement.

Ci = Cn* (Vn/Vo)*(Vo/Vi) where Cn*Vn is the total protein mass and Vi is the volume at the ith measurement.